Electrical and Thermal Properties of Bi_2Te_3

C. B. SATTERTHWAITE AND R. W. URE, JR.
Westinghouse Research Laboratories, Pittsburgh, Pennsylvania
(Received August 15, 1957)

Samples of both n-type and p-type Bi_2Te_3 containing from 3×10^{17} to 5×10^{19} extrinsic carriers were prepared and the phase diagram in the region about Bi_2Te_3 has been clarified. The Hall mobility parallel to the cleavage planes varies as $T^{-1.5}$ for holes and $T^{-2.7}$ for electrons. Room temperature values are $\mu_p=420$ cm^2 v^{-1} sec^{-1} and $\mu_n=270$ cm^2 v^{-1} sec^{-1}. The energy gap is $E_g=0.20$ electron volts. From thermal conductivity measurements over the temperature range from 77°K to 380°K the lattice conductivity was found to be $\kappa_L=5.10\times10^{-2}/T$ watt-deg^{-1} cm^{-1}. The sharp rise in the thermal conductivity in the vicinity of room temperature was attributed to transport of energy by ambipolar diffusion of electrons and holes.

I. INTRODUCTION

BISMUTH telluride recently has been of considerable interest, particularly as a thermoelectric material; however, the electrical and thermal properties of this material have not been established. The present paper describes the preparation of bismuth telluride of known composition and a study of the thermal conductivity and the electrical properties of both n- and p-type material.

II. PREPARATION

From the published phase diagram for the bismuth-tellurium[1] system it appears that the maximum in the liquidus curve should occur near 60 atomic percent Te. If, indeed, the maximum occurred at the stoichiometric composition, Bi_2Te_3, it should be possible to approach that composition by successive zone refining. Assuming that Bi_2Te_3 represents a composition in which the valence band is just filled successive zone-refining should produce a near intrinsic semiconductor.

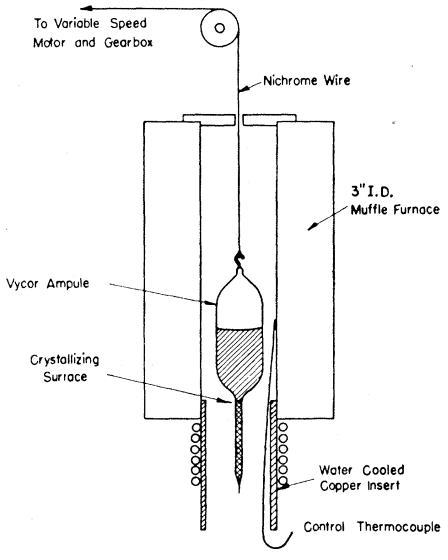

FIG. 1. Vertical crystal furnace.

[1] M. Hansen, *Der Aufbau der Zweistofflegierungen* (Verlag Julius Springer, Berlin, 1936).

This was found not to be the case. Whether the starting material contained an excess of Bi or an excess of Te the zone refined Bi_2Te_3 contained approximately 2×10^{19} excess holes.

By the technique described below the details of the phase diagram in the region of Bi_2Te_3 were clarified and also a series of single crystal samples of varying carrier concentration were produced for studies of the electrical and thermal properties.

Since in general, the composition of the liquid and solid in equilibrium are different, it is desirable, in order to obtain crystals of uniform composition, to crystalize from a very large melt so that the change in composition of the liquid during solidification of a small sample is negligible. It is also desirable to solidify very slowly so that the excess of one component rejected at the crystallizing surface diffuses uniformly throughout the melt. The apparatus for producing crystals under these conditions is shown in Fig. 1.

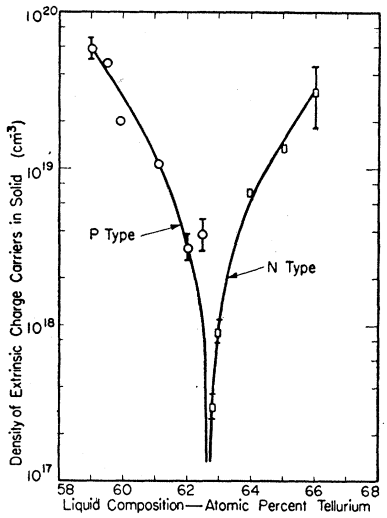

FIG. 2. Solid-liquid equilibrium composition. Solid composition is expressed in terms of the number of extrinsic charge carriers.

The starting materials were sufficiently pure that further purification was not needed. The bismuth was

obtained from Cerro de Pasco Corporation and by their analysis was 99.999% pure. The tellurium was American Smelting and Refining's "Special High Purity" grade which analyzed 99.999% pure. Bismuth and tellurium were weighed out to make a melt of approximately 80 g of the desired composition and sealed under high vacuum in a Vycor ampule shaped as shown in Fig. 1. After the materials had been melted and thoroughly mixed, the ampule was suspended in the crystal furnace and was lowered through a sharp temperature gradient at a rate of 1 to 3 inches in 24 hours. With the bottom of the tail section drawn down to a narrow cone single crystals or polycrystals with large single-crystal regions were formed.

Single-crystal samples were taken from the first gram solidified, and were considered to have been

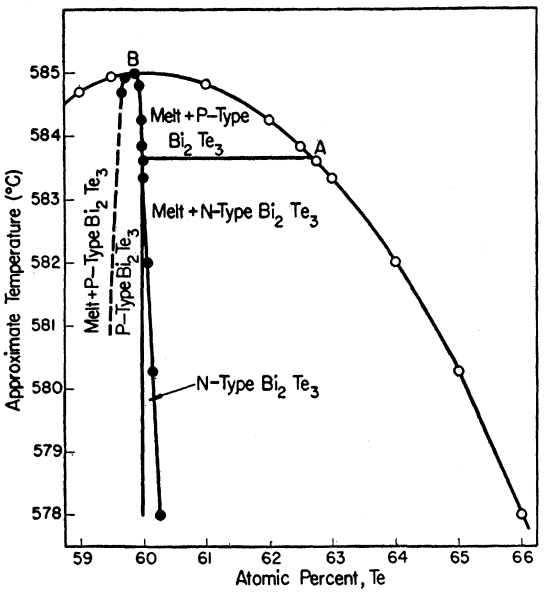

FIG. 3. Phase diagram for Bi—Te in the region about Bi_2Te_3. The composition of the solid was inferred from Hall effect measurements.

solidified under equilibrium conditions from a melt of the original composition. From liquid nitrogen Hall effect data on these samples, the number and kind of excess carriers were determined. Figure 2 shows the number of excess carriers as a function of melt composition.

If we assume that each excess Bi atom behaves as a singly ionized acceptor and each excess Te atom as a singly ionized donor, we can relate the carrier concentration to the concentration of excess Bi or Te atoms in the crystal. Thus, from the data shown in Fig. 2 and the average atomic volume, we can construct a phase diagram for the region about Bi_2Te_3. By estimating the shape of the liquidus curve and the temperature scale from the gross phase diagram,[1] the diagram shown in Fig. 3 was constructed. The room temperature

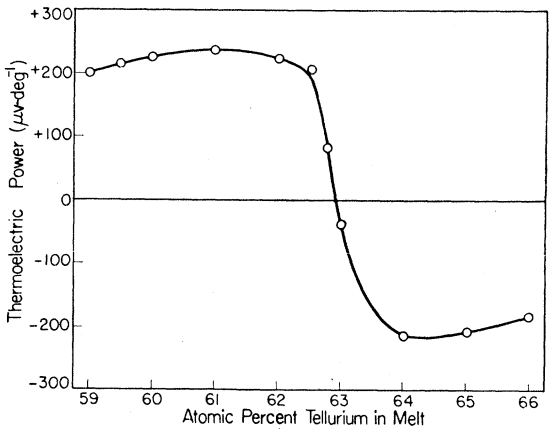

FIG. 4. Room temperature thermoelectric power of Bi_2Te_3 as a function of composition of liquid from which the crystals were grown.

thermoelectric power of the crystals as a function of melt composition, shown in Fig. 4, is consistent with this phase diagram. Goldberg and Mitchell[2] constructed a similar phase diagram for the Pb-Se system in the region of PbSe to explain their electrical data.

It may be noted that a melt of composition A, shown in Fig. 3, is in equilibrium with the stoichiometric compound Bi_2Te_3 at its melting point. Composition B represents a constant freezing composition which will be approached by successive zone meltings.

A study of the preparation of Bi_2Te_3 has been reported by Ainsworth.[3] The method he describes as the "Stockbarger Method" is similar to our method of preparation. He apparently made no effort to maintain the liquid volume large compared to the volume of the crystal so that one would expect large variations in the composition of the solid as solidification progressed except at the constant freezing composition. Since his starting compositions are not listed, it is difficult to compare results.

III. ELECTRICAL PROPERTIES

A. Experimental Procedure

Hall effect and resistivity were measured in two n-type and three p-type samples over a temperature range from 77°K to about 375°K. Rectangular samples were cut from the single crystals with the long axis of the rectangle parallel to the cleavage plane. The samples were about 2 cm long and from 0.10 to 0.25 cm in width and thickness. Current contacts were made to the ends of the samples by ultrasonic soldering techniques using pure tin as the solder. Potential contacts were made by pressing manganin wires against the specimen. Four probes were used; thus the Hall coefficient at two points on the sample and the

[2] A. E. Goldberg and G. R. Mitchell, J. Chem. Phys. **22**, 220 (1954).

[3] L. Ainsworth, Proc. Phys. Soc. (London) **B69**, 606 (1956).

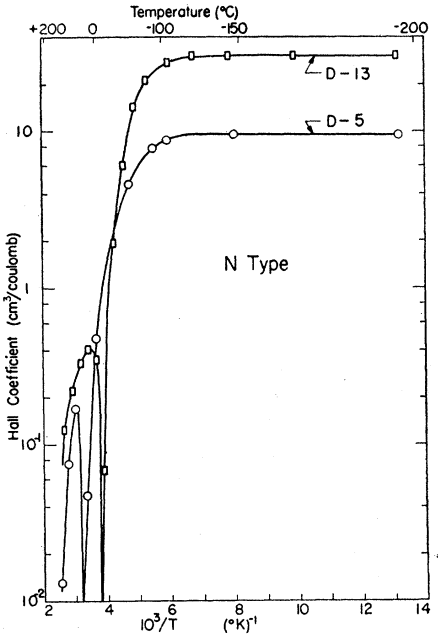

FIG. 5. Hall coefficient of n-type bismuth telluride samples. The current and Hall voltage were parallel to the cleavage plane and the magnetic field was perpendicular to the cleavage plane.

conductivity on each side of the sample was measured. The apparatus for maintaining constant uniform temperatures is described elsewhere.[4]

Because of the high thermoelectric effects and low thermal conductivity in Bi_2Te_3, the measuring current set up temperature gradients which produced appreciable thermoelectric voltages across the conductivity probes. To eliminate this voltage, one reading was taken after the current had established a steady state temperature distribution. A second reading was then taken immediately after reversing the current thus maintaining the same temperature distribution for the two readings. The resistivity was calculated from the average of the two readings. By a similar procedure with magnetic field on, it was found that the voltages due to the Ettingshausen and Nernst effects were negligible compared to the Hall voltage.

Because of the method of preparation one would expect the composition to change slightly along the direction of growth. In most of the samples the Hall coefficient was somewhat different on the two sets of probes indicating some inhomogeneity of this sort. The magnitude of the inhomogeneity is shown by the length of the vertical lines on Fig. 2.

Bismuth telluride is quite anisotropic. It has a hexagonal lattice with space group $R3m$. Voigt[5] has shown that the two independent components of the conductivity tensor are the conductivity perpendicular to and parallel to the cleavage plane and that there are two independent components of the Hall coefficient tensor. In measurements of resistivity and Hall coefficient, all directions in the cleavage plane are equivalent.[6]

We have measured conductivities in the direction parallel to the cleavage plane. Measurements of Hall coefficients were made with magnetic field perpendicular to the cleavage plane and electric current and Hall voltage parallel to cleavage plane. On one sample the Hall coefficient was also measured with the magnetic field and current parallel to the cleavage plane and the Hall voltage perpendicular to the cleavage plane.

B. N-Type Samples

The Hall coefficients R of the n-type samples are shown in Fig. 5. For both samples the Hall coefficient changes sign as the intrinsic temperature range is approached. The change in sign occurs at 270°K for sample D-13 and 320°K for sample D-5. This shows

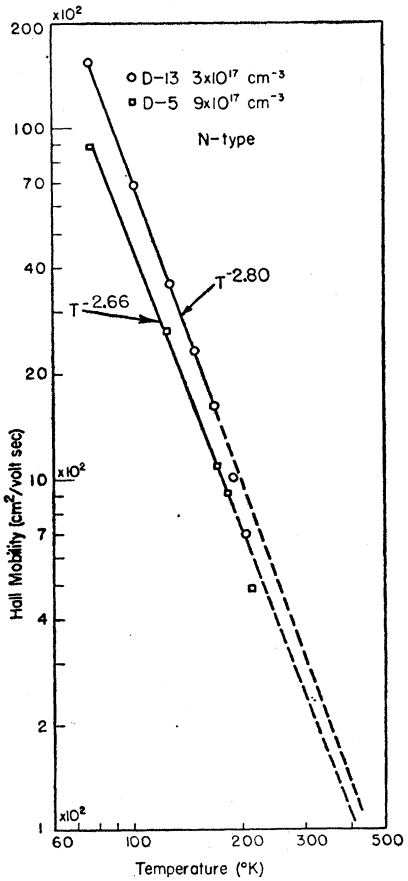

FIG. 6. Hall mobility ($\mu_H = R/\rho$) of two n-type bismuth telluride samples. The Hall coefficient was measured with the current parallel to cleavage plane and magnetic field perpendicular to cleavage plane. The resistivity was measured parallel to the cleavage plane.

[4] R. W. Ure, Jr., Rev. Sci. Instr. **28**, 836 (1957).

[5] W. Voigt, *Lehrbuch der Kristallphysik* (B. G. Teubner, Leipzig, 1910).

[6] J. R. Drabble and R. Wolfe, Proc. Phys. Soc. (London) **B69**, 1101 (1956).

that the hole mobility is larger than the electron mobility in this range of temperature.

The electron Hall mobility ($\mu_H=R/\rho$) of two samples is shown in Fig. 6. The average value is $\mu_n=1.35\times10^9\ T^{-2.7}$ cm²/v sec. The hole mobility at the temperature at which $R=0$ can be calculated from a knowledge of this temperature and the values of ρ and μ_n. The ratio of the mobilities is then given by[7]

$$\mu_n/\mu_p=(\rho_e-\rho_0)/\rho_e,$$

where ρ_e is the extrapolated low-temperature resistivity and ρ_0 is the actual resistivity both at the temperature at which the Hall coefficient is zero. The hole mobilities determined in this way were extrapolated to 300°K using the temperature dependence of the hole mobility as determined on p-type samples. The values are shown in Table I.

C. *P*-Type Samples

The Hall coefficient of several p-type samples is shown in Fig. 7, and the Hall mobility is shown in Fig. 8. The values of both components of the Hall effect tensor were measured on sample *D*-7. The ratio of the two components is 1.4 in the temperature range from 77°K to 200°K. The Hall coefficient with magnetic field and electric current parallel to the cleavage plane is the larger of the two coefficients.

TABLE I. Hall mobilities (R/ρ) for Bi_2Te_3 as reported by various investigators. In this work, the resistivity was measured in the direction parallel to the cleavage plane, and the Hall constant was measured with the current parallel to the cleavage plane and the magnetic field perpendicular to the cleavage plane. The differences in the 300°K Hall mobility values may be due to different investigators using different sample orientations to measure the Hall effect.

	μ_p at 300°K (cm²/v sec)	Temperature dependence of μ_p	μ_n at 300°K (cm²/v sec)	Temperature dependence of μ_n	Density of extrinsic carriers (cm⁻³)	Energy gap (ev)
This work:						
n-type samples						
D-5	330		240	$T^{-2.66}$	9×10^{17}	
D-13	440		310	$T^{-2.80}$	3×10^{17}	0.20
p-type samples						
Zone refined	410	$T^{-1.4}$			2×10^{19}	
D-4	430	$T^{-1.60}$			3×10^{18}	
D-7	680	$T^{-1.8}$			4×10^{18}	
Wright[a]	325	$T^{-1.5}$	250	$T^{-1.5}$	...	
Shigetomi and Mori[b]	280	$T^{-2.3}$			1.4×10^{19}	0.21
Black, Conwell, Seigle, and Spencer[c]	400	$T^{-1.4}$			1×10^{19}	0.16
Harman, Paris, Miller, and Goering[d]	400				8×10^{18}	0.16
			180[e]		...	
			540[f]		5×10^{18}	

[a] D. A. Wright, reported at International Conference on Semiconductors, 1956 (unpublished).
[b] See reference 9.
[c] See reference 11. These authors used the same sample orientation as ours.
[d] See reference 10.
[e] From Fig. 13, reference 10.
[f] From Table I, reference 10.

[7] W. Shockley, *Electrons and Holes in Semiconductors* (D. Van Nostrand Company, Inc., New York, 1950), p. 218.

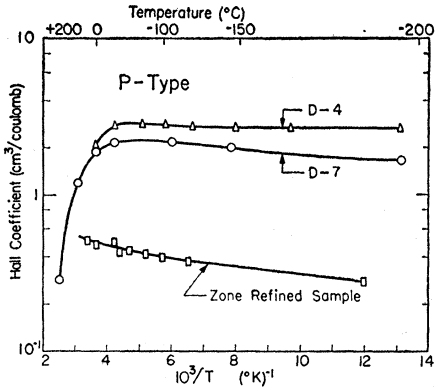

FIG. 7. Hall coefficient of p-type bismuth telluride samples. The current and Hall voltage were parallel to the cleavage plane and the magnetic field was perpendicular to the cleavage plane.

D. Intrinsic

The condition for electrical neutrality in an n-type sample is $p=n-n_s$ when n and p are the density of electrons and holes and n_s is the density of uncompensated donors. From this equation and the equation for the electrical conductivity, $\sigma=e(n\mu_n+p\mu_p)$, one finds

$$n=\frac{1}{\rho e(\mu_p+\mu_n)}+\frac{n_s\mu_p}{\mu_p+\mu_n}. \qquad (1)$$

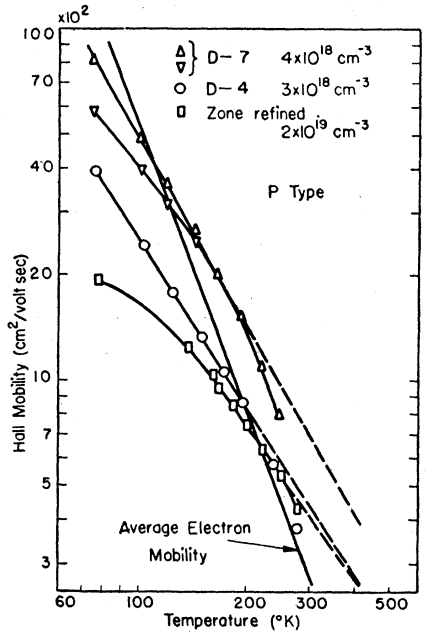

FIG. 8. Hall mobility ($\mu_H=R/\rho$) of three p-type bismuth telluride samples. The Hall coefficient was measured with the current parallel to the cleavage plane and the magnetic field perpendicular to the cleavage plane. The two curves for sample *D*-7 were calculated from conductivity data taken on opposite sides of the sample and show rather large inhomogeneity in the sample. The resistivity was measured parallel to the cleavage plane.

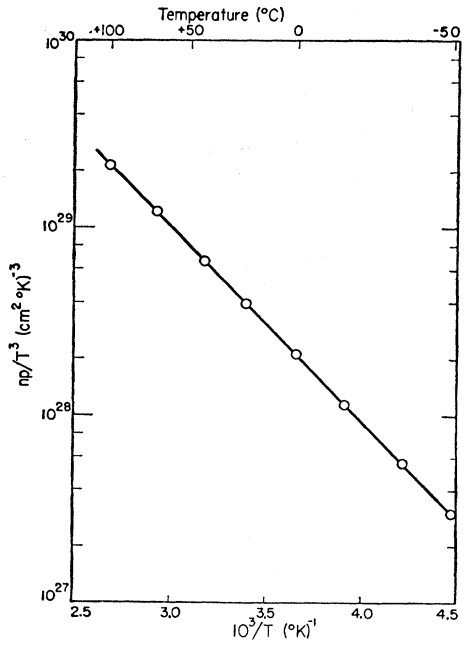

FIG. 9. Product of electron and hole density divided by temperature cubed as a function of reciprocal temperature.

The number of electrons and holes in sample D-13 was calculated using the extrapolated low-temperature values of μ_n and measured values of ρ. The values of μ_p were the extrapolated low-temperature values for sample D-4. The value of n_s was taken from low-temperature Hall effect data. In Fig. 9, the value of $\ln(np/T^3)$ is plotted against $1/T$. The energy gap is given by the slope of this curve,[8] and is $E_g=0.20$ ev.

E. Discussion

As shown in Table I, several other investigators have reported data on Bi_2Te_3. If different sample orientations were used to measure the Hall effect, their results should differ from ours. Our data on the anisotropy of the Hall coefficient in p-type material indicate that the component of the Hall effect tensor which we used to calculate Hall mobilities is the smaller of the two components in p-type material. Hence our Hall mobility values calculated on p-type samples are smaller than those calculated from the other component of the Hall effect tensor.

Measurements[9–11] on p-type samples having excess donor concentrations from 8×10^{18} to 2×10^{19} cm^{-3} have shown a reversal in sign of the Hall effect and thermoelectric power as the samples become intrinsic at temperatures of 435 to 525°K. This shows that the electron mobility is higher than the hole mobility in this high-temperature range. Our n-type samples D-5 and D-13 have a smaller excess carrier concentration and hence become intrinsic at a much lower temperature. The Hall effect in these samples changes sign from n type to p type as they become intrinsic showing that the hole mobility is larger than the electron mobility in the temperature range about 270 to 320°K. Our measurements and other direct measurements of the Hall mobility of electrons in n-type material and holes in p-type material show that the hole mobility is indeed higher than the electron mobility near 300°K. The only values of 300°K electron mobility reported in the literature which are higher than the 300°K hole mobility (400 cm^2/v sec) are values calculated from the high-temperature reversal of p-type samples and some of the values of Harman, Paris, Miller, and Goering.[10] To account for this reversal of the Hall effect in p-type samples at high temperature, the temperature variation of one or both of the mobilities must deviate from the simple power law found below room temperature in such a way that the electron mobility exceeds the hole mobility at high temperatures.

IV. THERMAL CONDUCTIVITY

The apparatus for making thermal conductivity measurements is shown schematically in Fig. 10. The method involved supplying heat at a measured rate to one end of a sample of uniform cross section and measuring the temperature difference between the ends by means of thermocouples. The transfer of heat by radiation or by conduction along the electrical leads was minimized by surrounding the sample with

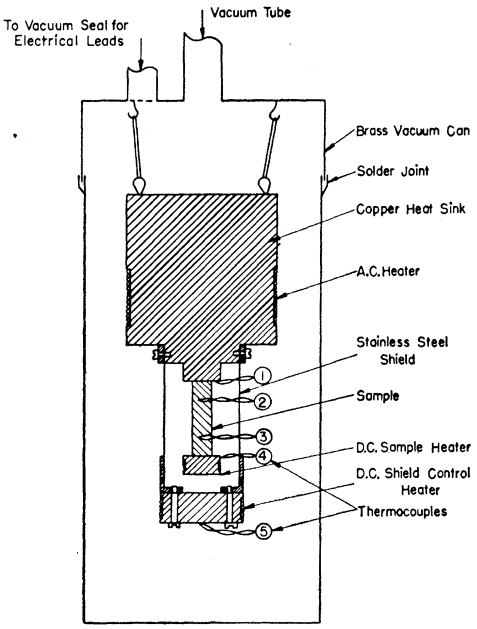

FIG. 10. Thermal conductivity apparatus.

[8] Reference 7, p. 245.
[9] S. Shigetomi and S. Mori, J. Phys. Soc. Japan **11**, 915 (1956).
[10] Harman, Paris, Miller, and Goering, J. Phys. Chem. Solids **2**, 181 (1957).
[11] Black, Conwell, Seigle, and Spencer, J. Phys. Chem. Solids **2**, 240 (1957).

a thermal shield. The thermal conductivity was then given by

$$\kappa=(P/\Delta T)(l/a), \qquad (2)$$

where P is the power, ΔT the temperature difference between the ends of the sample, l the length, and a the cross-sectional area. At each temperature a steady state was reached with the system isolated by vacuum (the heat sink was massive enough so that the heat supplied to it through the sample and shield increased its temperature only infinitesimally). The heat supplied to the shield heater was adjusted to maintain its temperature equal to the temperature of the sample heater. Heat flow along the electrical leads was minimized by thermally bonding each lead to the shield at a point corresponding in temperature to its point of contact on the sample.

The thermocouples were of Cu-Constantan and were calibrated at four fixed points, the N_2 boiling point, the CO_2 sublimation point, the ice point, and the steam point.

Measurements were made on two single crystalline samples, one prepared by zone melting and containing 2×10^{19} excess holes per cm^3 and the other prepared by the method described in Sec. II and containing 3×10^{17} excess electrons per cm^3. The samples were both approximately $0.5\times0.5\times2.5$ cm rectangular solids with the long dimension parallel to the cleavage planes, i.e., in the direction of growth. The samples were soldered to the heat sink and the sample heater with pure tin using ultrasonic soldering techniques. From initial measurements the thermal conductivity was calculated both from thermocouples 2 and 3 (see Fig. 10) with an effective length equal to the distance between them and also from 1 and 4 with an effective length equal to the length of the sample. Since these agreed throughout the temperature range, thermocouples 2 and 3 were eliminated for subsequent measurements.

The vacuum chamber was immersed in a bath of liquid N_2, CO_2-acetone, ice, or water depending upon the temperature range desired. The fact that the bath temperature sometimes differed appreciably from the temperature of measurement apparently did not introduce errors in the measurements. In the temperature region between liquid N_2 and CO_2 and again in the region between CO_2 and ice, points taken using the lower temperature bath were duplicated using the higher temperature one. Although the temperature drifts were in opposite directions, the results were essentially identical.

The thermal conductivity data for both samples are shown in Fig. 11 (a) together with curves for two samples of Goldsmid's.[12] In materials containing free carriers, heat is carried both by the free carriers and by the lattice phonons and these contributions to the thermal conductivity are additive. At low temperatures

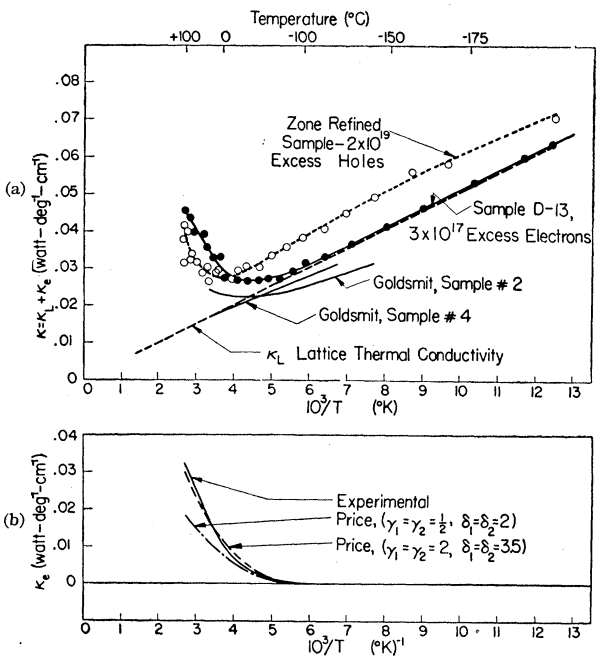

FIG. 11. (a) Thermal conductivity of two samples of Bi_2Te_3 together with representative data of Goldsmid. (b) Thermal conductivity due to the free carriers in the near intrinsic sample, D-13. Carrier conductivity calculated on the basis of Price's theory with two assumed sets of values for the scattering parameters are shown for comparison.

the contribution due to the free carriers can be calculated from the electrical resistivity. This calculation may be somewhat uncertain in semiconductors since it depends upon the type of scattering of the carriers and their degree of degeneracy. The thermal conductivity of the Bi_2Te_3 lattice was calculated from low-temperature data on sample D-13. In this sample at low temperatures the carrier thermal conductivity was small because of the small carrier concentration. The lattice thermal conductivity varies as $1/T$ as predicted by theory and is given by

$$\kappa_L=5.10\times10^{-2}/T \text{ watt/deg cm.}$$

The sharp rise in the thermal conductivity at the higher temperatures is believed to arise largely from the transport of gap energy by ambipolar diffusion. A quantitative treatment of this phenomenon has been given by Price.[13] In order to compare our data on sample D-13 with his theory it is necessary to assume that the lattice thermal conductivity remains linear in $1/T$ throughout the temperature range. The expression he gives for the carrier thermal conductivity is

$$\kappa_e=\sigma T(k/e)^2(\Omega+\Omega_0), \qquad (3)$$

where

$$\Omega(T)=\frac{\sigma_n\sigma_p}{\sigma^2}\{(E_g/kT)^2+\alpha(E_g/kT)+\beta\}, \qquad (4)$$

[12] H. J. Goldsmid, Proc. Phys. Soc. (London) **B69**, 203 (1956).

[13] P. J. Price, Phil. Mag. **46**, 1252 (1955).

Ω_0 is the coefficient relating the normal thermal conductivity of the individual bands to the electrical conductivity, and σ_n and σ_p represent the electrical conductivity of the holes and electrons separately, i.e. $\sigma_n=ne\mu_n$ and $\sigma_p=pe\mu_p$. The coefficients α and β depend on the relaxation processes and are related to the γ's and δ's, defined by Price's Eqs. (4) and (11), in the following way:

$$\alpha=\delta_n+\delta_p+3+\gamma_n+\gamma_p, \tag{5}$$

and

$$\beta=(3+\gamma_n+\gamma_p)(\delta_n+\delta_p). \tag{6}$$

If the carriers of both bands may be treated by Boltzmann statistics and if the carrier mean free path is determined by lattice scattering, $\Omega_0=2$, $\gamma_n=\gamma_p=\frac{1}{2}$ and $\delta_n=\delta_p=2$. More generally, if the scattering obeys a power law, i.e., the relaxation time is proportional to the mth power of the electron energy ($\tau\sim E^m$), and the carriers still obey Boltzmann statistics

$$\gamma=1+m \quad \text{and} \quad \delta=\tfrac{5}{2}+m.*$$

The contribution to the thermal conductivity in the intrinsic region due to the free carriers was obtained for samples *D*-13 by subtracting the lattice contributions from the measured conductivity. This is shown in Fig. 11 (b) together with two curves constructed from Price's expression Eq. (3), one assuming conventional lattice scattering with $\gamma_n=\gamma_p=\frac{1}{2}$ and $\delta_n=\delta_p=2$ and the other assuming $\gamma_n=\gamma_p=2$ and $\delta_n=\delta_p=3.5$.

Through there is qualitative agreement between experimental and theoretical curves they differ appreciably. Better agreement is obtained if the larger values of the γ's and δ's are assumed. However, the experimental curve rises more sharply with temperature than the theoretical curve with any reasonable choice of γ's and δ's. In his treatment, Price has made a number of assumptions, such as cubic symmetry and single energy minima in both the valence and conduction bands, which are not strictly applicable to bismuth telluride. Therefore exact agreement between theory and experiment would not be expected.

Other mechanisms for additional heat transport in semiconductors have been suggested,[14] for example, transport by excitons and phonon drag by either electron-hole pairs or excitons. The exciton hypothesis has been useful in explaining the thermal conductivity of PbTe. In Bi_2Te_3 the anomalous thermal conductivity occurs at the right temperature for ambipolar diffusion so that any other mechanism would be difficult to identify without additional evidence.

No quantitative treatment was made of the highly doped *p*-type sample. However, it can be seen that it exhibits similar behavior. The sharp rise occurs at a higher temperature as would be expected for a more highly doped sample and the conductivity increases more rapidly. The differences between the two samples at low temperatures can be explained by the difference in the normal carrier thermal conductivity as estimated from the electrical conductivity.

V. ACKNOWLEDGMENTS

The authors wish to express their appreciation to Mr. John Gavaler for his assistance with the preparation and measurements and to Dr. R. W. Keyes for suggestions about treatment of the results.

* *Note added in proof.*—Price has shown that as a result of the Onsager reciprocal relationships there is a general relationship between γ and δ; i.e., $\delta=\gamma+\frac{3}{2}$ [P. J. Price, Phys. Rev. **104**, 1227 (1956)].

[14] A. F. Joffe, Can. J. Phys. **34**, 1342 (1956).